

The Capacitance and Electromechanical Coupling of Lipid Membranes Close to Transitions: The Effect of Electrostriction

Thomas Heimburg*

The Niels Bohr Institute, University of Copenhagen, Copenhagen, Denmark

ABSTRACT Biomembranes are thin capacitors with the unique feature of displaying phase transitions in a physiologically relevant regime. We investigate the voltage and lateral pressure dependence of their capacitance close to their chain melting transition. Because the gel and the fluid membrane have different area and thickness, the capacitance of the two membrane phases is different. In the presence of external fields, charges exert forces that can influence the state of the membrane, thereby influencing the transition temperature. This phenomenon is called “electrostriction”. We show that this effect allows us to introduce a capacitive susceptibility that assumes a maximum in the melting transition with an associated excess charge. As a consequence, voltage regimes exist in which a small change in voltage can lead to a large uptake of charge and a large capacitive current. Furthermore, we consider electromechanical behavior such as pressure-induced changes in capacitance, and the application of such concepts in biology.

INTRODUCTION

Biological membranes provide a barrier between cells and organelles that serves to maintain differences in chemical and electrical potentials by separating molecules and ions. The electrical phenomena that result from transient changes in these electrochemical potentials provide the basis for contemporary understanding of the electrophysiology of biomembranes (1,2). The cell membrane consists mainly of a lipid bilayer into which proteins are embedded. It is widely (but incorrectly (see (49))) believed that the lipid bilayer itself is impermeable to water, ions, and molecules. Therefore, electrophysiology considers the membrane to be a capacitor, and ion channel proteins are regarded as electrical resistors. The nerve pulse, for instance, is considered as a propagating segment of charged capacitor loaded by currents through the channel proteins (3).

The membrane capacitance, C_m , defines how much charge, q , is stored on two capacitor plates at a fixed membrane voltage, V_m ,

$$q = C_m \cdot V_m. \quad (1)$$

For a parallel plate capacitor, C_m is given by

$$C_m = \epsilon_0 \epsilon \frac{A}{D}, \quad (2)$$

with vacuum permittivity $\epsilon_0 = 8.85410^{-12}$ F/m and dielectric constant $\epsilon \approx 2-4$. Here, A is the area of the membrane, and D is its thickness.

Excitatory processes in cells are typically accompanied by changes in voltage. During nerve pulses, for instance, the voltage changes transiently by ~ 100 mV in 1 ms. Volt-

ages as large as 100 mV are also typical in the voltage-clamp experiments that are used to measure protein conductances (4). In electroporation experiments, used to transport drugs or DNA into cells, voltages can be on the order of several 100 mV (5,6). Stimulation voltages for nerve pulses can be of order up to 1 V (e.g., Kassahun et al. (7)).

A change in voltage leads to a capacitive current because the charge on the capacitor changes. The capacitive current induced by a change in voltage is given as

$$\frac{dq}{dt} = \frac{d}{dt}(C_m \cdot V_m) = C_m \frac{dV_m}{dt} + V_m \frac{dC_m}{dt}. \quad (3)$$

In electrophysiological models such as the Hodgkin-Huxley model for nerve pulse propagation and in the interpretation of voltage-clamp experiments, it is assumed that the capacitance of biomembranes (in particular of nerves) is independent of voltage (i.e., C_m is constant) so that the second term on the right of this equation is zero (e.g., Johnston and Wu (2) and Hodgkin and Huxley (3)). This is equivalent to assuming that membrane dimensions are unaffected by electrical phenomena and that the excitation of membranes does not change their dimensions. The second of these assumptions is known to be incorrect because changes in the thickness of nerve membranes during the action potential have been observed (8–14). Furthermore, there are numerous reports in the literature on voltage-induced changes in membrane bending, i.e., caused by flexoelectricity or mechanoelectricity (15–17). In the recent years, we have proposed that the voltage changes during the nerve pulse are actually related to changes in capacitance (13,18–22).

In this article, we show that the assumption of constant capacitance is incorrect, especially if one is close to chain melting transitions in the lipid membrane. Biological membranes display transitions close to physiological temperature. Heat capacity maxima are typically found

Submitted May 29, 2012, and accepted for publication July 10, 2012.

*Correspondence: theimbu@nbi.dk

Editor: Paulo Almeida.

© 2012 by the Biophysical Society
0006-3495/12/09/0918/12 \$2.00

<http://dx.doi.org/10.1016/j.bpj.2012.07.010>

10–15° below physiological or growth temperature, both for bacterial membranes from *Escherichia coli* and *Bacillus subtilis*, for lung surfactant (13) and for nerves from the spine of rats (S. B. Madsen and N. V. Olsen, unpublished data). The fluid state membrane is thinner than the gel membrane. Simultaneously, the area of the fluid membrane is larger (23). This implies that the capacitance of the fluid membrane is larger than that of the gel membrane. Thus, any phenomenon in the biomembrane related to a phase transition will influence its capacitance. For instance, the temperature of the phase transition is influenced by charges on the capacitor because electrostatic forces act on the capacitor plates. Further, hydrostatic pressure (24), lateral pressure (13), or the addition of drugs like anesthetics (25) influence the position of the melting transition. Therefore, the capacitance must be also a function of voltage, hydrostatic pressure, lateral pressure, and the concentration of anesthetics.

We show here that close to a transition voltage is able to change the dimensions of a membrane and the capacitance. We also show how the electrical properties of the membrane are affected by the application of lateral pressure or tension in a membrane. This gives rise to pressure-induced capacitive currents or pressure-induced voltage changes. Although we restrict ourselves primarily to the phenomenon of electrostriction, i.e., the force that capacitive charges exert on the capacitor, we also discuss polarization effects.

THEORY

Consider a capacitor whose equilibrium properties depend on voltage V_m only, i.e., all other intensive variables of the system such as pressure and temperature are kept constant. We write

$$dq = \left(\frac{\partial q}{\partial V_m} \right) dV_m \equiv \widehat{C}_m dV_m. \quad (4)$$

Here we introduce the function $\widehat{C}_m = (\partial q / \partial V_m)$, which we call the “capacitive susceptibility”. Note that the definition of \widehat{C}_m differs from that of the capacitance that is given by $C_m = q/V_m$. According to Eq. 1, Eq. 4 corresponds to

$$\begin{aligned} dq &= \left(\frac{\partial(C_m V_m)}{\partial V_m} \right) dV_m = \left(C_m + V_m \frac{\partial C_m}{\partial V_m} \right) dV_m \\ &= C_m dV_m + V_m dC_m. \end{aligned} \quad (5)$$

This equation takes into account that the changes of the charge on a capacitor are not solely due to voltage changes but also to voltage-induced changes in capacitance, which are described by the capacitive susceptibility

$$\widehat{C}_m \equiv C_m + V_m \frac{\partial C_m}{\partial V_m}. \quad (6)$$

If the capacitance C_m is independent of voltage, we obtain $\widehat{C}_m = C_m$. However, the last term on the right-hand side

of Eq. 6 can become large close to transitions in biomembranes, as we will show below. In the context of transitions, this term can be considered an excess capacitance. It is proportional to the voltage. Therefore, it is zero at zero voltage where the capacitor is not charged. In contrast, the function C_m has a finite value because it depends only on the dimensions of the capacitor.

The capacitive susceptibility \widehat{C}_m is fully analogous to other susceptibilities such as heat capacity, $(dH/dT)_P$, isothermal volume compressibility, $-(dV/dp)_T$, and isothermal area compressibility, $-(dA/d\Pi)_T$. The capacitive susceptibility has been used before, e.g., by Carius (26).

Electrostriction

Electrostriction is the generation of a mechanical force on a capacitor by the electrostatic attraction of the charges on the two capacitor plates. In the absence of other forces, increasing the voltage on a capacitor will generally tend to deform the capacitor such that its thickness is reduced.

Consider a membrane with fixed thickness D , a capacitance C_m (given by Eq. 2), and a transmembrane voltage, V_m . The field across the membrane is $E = V_m/D$ (assuming a uniform dielectric constant in the membrane interior), and the charge is $q = C_m V_m$. The force, \mathcal{F} , acting on this capacitor is given by Vanselow (27) as

$$\mathcal{F} = \frac{1}{2} E \cdot q = \frac{1}{2} \frac{V_m}{D} q = \frac{1}{2} \frac{C_m V_m^2}{D}. \quad (7)$$

The force \mathcal{F} and the field E are vectors normal to the membrane surface. Assuming that the fluid membrane has a capacitance of $C_m = 0.5 \mu\text{F}/\text{cm}^2 = 0.5 \cdot 10^{-2} \text{ F}/\text{m}^2$, this results in a pressure on the membrane of $p = 10^4 \text{ N}/\text{m}^2$ at 100 mV, which corresponds to 0.1 bar. Due to its quadratic dependence on voltage, this pressure is 100 times larger ($p = 10 \text{ bar}$) at $V_m = 1 \text{ volt}$. In contrast to hydrostatic pressure, this pressure has a direction normal to the membrane. This implies that increasing this force results in a reduction of thickness and an increase in area. Because the melting of a membrane is linked to an increase in area, an increase of transmembrane voltage can therefore potentially melt a membrane.

At constant voltage, the work done by the electrical field upon melting of the membrane is given by

$$\Delta W_c = \int_{D_g}^{D_f} \mathcal{F} dD = \frac{1}{2} \epsilon_0 V_m^2 \int_{D_g}^{D_f} \epsilon \frac{A}{D^2} dD, \quad (8)$$

where D_g and D_f are the thickness of the gel and the fluid membrane, respectively. For constant area, this relation yields the familiar expression for the work done on a capacitor, $1/2 C_m V_m^2$. However, the membrane area does not stay constant here.

The area in the fluid state of 1,2-dipalmitoyl-*sn*-3-phosphatidylcholine (DPPC) is 24.6% larger than in the gel state and the thickness is 16.3% smaller (24). If we assume a dielectric constant ϵ independent of voltage and membrane state, this difference is

$$C_m^{fluid} = \epsilon_0 \epsilon \frac{A_g \cdot (1 + 0.246)}{D_g \cdot (1 - 0.163)} = 1.49 C_m^{gel}. \quad (9)$$

Thus, the capacitance in the fluid phase is ~ 1.5 times larger than that of the gel phase, and the force across the membrane is 1.78 times larger than in the gel phase. In the presence of a voltage difference, a sudden change in membrane state can lead to significant capacitive currents (see Discussion).

The assumption made above of a voltage- and temperature-independent dielectric constant may not be correct. Paraffin oil has a dielectric constant of 2.2–4.7 and olive oil has 3.1 whereas paraffin wax has 2.1–2.5 (Dielectric Constants Chart; ASI Instruments, Warren, MI). Therefore, it may be possible that the dielectric constant in the fluid membrane is somewhat higher. Lacking reliable data for membranes, we consider ϵ to be constant.

Voltage dependence of the melting temperature

In the following, we describe the melting of a membrane in the presence of a transmembrane voltage. We approximate the excess heat capacity in the absence of voltage, $\Delta c_{p,0} = d(\Delta H_0(T))/dT$, by assuming that the transition is governed by a van't Hoff law, i.e., by a two-state transition from gel to fluid with a temperature-dependent equilibrium constant $K(T)$. The temperature dependence of the excess enthalpy, $\Delta H_0(T)$, is given by

$$\Delta H_0(T) = \frac{K(T)}{1 + K(T)} \Delta H_0$$

with

$$K(T) = \exp\left(-n \cdot \frac{\Delta H_0}{k} \left(\frac{1}{T} - \frac{1}{T_m}\right)\right), \quad (10)$$

where n is a cooperative unit size that determines how many lipids undergo a transition at the same time. For DPPC, the total excess enthalpy of the transition is $\Delta H_0 = 39$ kJ/mol, and the melting temperature is $T_m = 314.2$ K. The transition of DPPC unilamellar vesicles is reasonably well described by $n = 100$. (For details of this calculation, see Heimburg (29).)

We denote the membrane volume as $V(T) = V_g + \Delta V(T)$ and the membrane area as $A(T) = A_g + \Delta A(T)$, where V_g and A_g are the volume and the area of the gel state lipids, and $\Delta V(T)$ and $\Delta A(T)$ are the temperature-dependent changes due to melting. In previous publications we have shown that the changes in both volume and area are proportional

to the excess enthalpy during the chain melting transition (23,24),

$$\begin{aligned} \Delta V(T) &= \gamma^V \Delta H_0(T), \\ \Delta A(T) &= \gamma^A \Delta H_0(T), \end{aligned} \quad (11)$$

where $\gamma^V = 7.8 \cdot 10^{-10}$ m³/J is a constant that is practically independent of the lipid species or the lipid mixture (24), and $\gamma^A = 0.89$ m²/J. We assume that a similar relation holds for the mean thickness,

$$\Delta D(T) = \gamma^D \Delta H_0(T), \quad (12)$$

with $\gamma^D = 2.49 \cdot 10^{-14}$ m/J. The thickness of the gel phase membrane, D_g , is 4.79 nm (for DPPC), and it is $D_f = 3.92$ nm in the fluid phase. DPPC in the gel phase has an area of $A_g = 0.474$ nm² per lipid and a membrane area $1.43 \cdot 10^5$ m² per mol of lipid (23). Here and below we will assume that the above proportionality to the enthalpy is valid. Further, we assume that the voltage dependence of the pure lipid phases is small.

According to Eq. 8, the enthalpy change, $\Delta H_0(T)$, at constant voltage, V_m , of the membrane at temperature, T , is given by

$$\begin{aligned} \Delta H(V_m, T) &= \Delta H_0(T) + \frac{1}{2} \epsilon_0 V_m^2 \int_{D_g}^{D(T)} \epsilon \frac{A(T)}{D(T)^2} dD \\ &= \Delta H_0(T) + \frac{1}{2} \epsilon_0 V_m^2 \int_0^{\Delta H_0(T)} \epsilon \frac{(A_g + \gamma_A \Delta H_0(T))}{(D_g + \gamma_D \Delta H_0(T))^2} \\ &\quad \times \gamma_D d\Delta H_0(T). \end{aligned} \quad (13)$$

Making use of $(1+x)^{-2} \approx 1 - 2x$ for small x and assuming constant ϵ , we finally obtain

$$\begin{aligned} \Delta H(V_m, T) &= \Delta H_0(T) \left(1 + \frac{1}{2} \epsilon_0 \epsilon \gamma_D V_m^2 \frac{A_g}{m D_g^2} \right. \\ &\quad \left. \times \left[1 + \frac{1}{2} \left(\frac{\gamma_A}{A_g} - 2 \frac{\gamma_D}{D_g} \right) \Delta H_0(T) \right] \right), \end{aligned} \quad (14)$$

where $\Delta H_0(T)$ is the temperature-dependent enthalpy in the absence of voltage described by Eq. 10. One can now determine the temperature dependence of $\Delta H(V_m, T)$. For $T \gg T_m$, $\Delta H(V_m, T)$ assumes a constant value, which is the excess heat of melting. It is a quadratic function of voltage: $\Delta H(V_m) = \Delta H_0 + \alpha_0 V_m^2$ with $\alpha_0 = 141.7$ [J/V²] using $\epsilon = 4$.

The value ΔH_0 is the melting enthalpy of the membrane in the absence of voltage with melting temperature $T_{m,0} = \Delta H_0/\Delta S_0$, and $\Delta H(V_m)$ is the melting enthalpy of the membrane with voltage V_m . The transition temperature T_m in the presence of voltage can be written as

$$\begin{aligned}
 T_m &= \frac{\Delta H(V_m)}{\Delta S_0} = \frac{\Delta H_0 + \alpha_0 V_m^2}{\Delta S_0} \\
 &= T_{m,0} + \frac{\alpha_0}{\Delta S_0} V_m^2 \equiv (1 + \alpha V_m^2) T_{m,0},
 \end{aligned} \quad (15)$$

with $\alpha = \alpha_0/\Delta H_0 = -0.003634 [1/V^2]$, and $\Delta S_0 = \Delta H_0/T_{m,0}$. The melting profiles and the melting temperature as a function of voltage are shown in Fig. 1. One obtains a shift of the transition temperature toward lower temperatures of -11.4 mK for $V_m = 100$ mV, of -1.14 K for $V_m = 1$ V, and of -114 K for $V_m = 10$ V. The effect of electrostriction on the melting temperature is obviously small at physiological voltages. However, it is large for voltages of >1 V.

The above calculation applies to a symmetric membrane. According to the results of Alvarez and Latorre (30), the quadratic voltage dependence of T_m can be shifted on the voltage axes when the membrane is asymmetrically charged. In this case, the maximum melting temperature can be achieved for voltages different than zero.

Voltage and temperature dependence of the capacitive susceptibility

It has been shown that outside of transitions, capacitance changes induced by voltage are small (31–33) but quadratic in voltage. As above, we will therefore assume that the

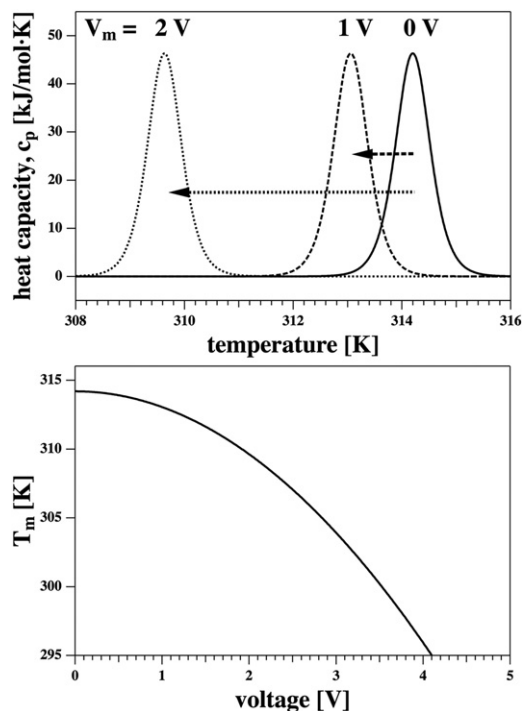


FIGURE 1 Influence of electrostriction on the melting of membranes. (Top) Excess heat capacity of DPPC large unilamellar vesicles (LUVs) at three different voltages. (Bottom) Change of the transition temperature of DPPC as a function of voltage (see Eq. 15).

voltage dependence of the capacitance in the transition regime is much higher than that of the pure phase. I.e., we assume that A_g and A_f as well as D_g and D_f display a negligible voltage dependence.

The charge on a membrane at temperature T and voltage V_m is then given by

$$q(V_m, T) = \epsilon \epsilon_0 \frac{A_{gel} + \Delta A(V_m, T)}{D_{gel} + \Delta D(V_m, T)} V_m, \quad (16)$$

and at voltage $V_m + dV$ by

$$q(V_m + dV_m, T) = \epsilon \epsilon_0 \frac{A_{gel} + \Delta A(V_m + dV_m, T)}{D_{gel} + \Delta D(V_m + dV_m, T)} \cdot (V_m + dV_m), \quad (17)$$

where ΔA and ΔD are again proportional to ΔH (see Eq. 14). For fixed voltage, the capacitance is a function of temperature only. For fixed temperature, it is a function of voltage only. The area and thickness of the membrane at $T = 311$ K are shown as a function of voltage in Fig. 2 (left).

The capacitive susceptibility, \hat{C}_m , is now given by

$$\hat{C}_m = \frac{dq}{dV_m} = \frac{q(V_m + dV_m, T) - q(V_m, T)}{dV_m}. \quad (18)$$

If the temperature T is below the melting temperature, $T_{m,0}$, voltage can induce a transition in the membrane. The value

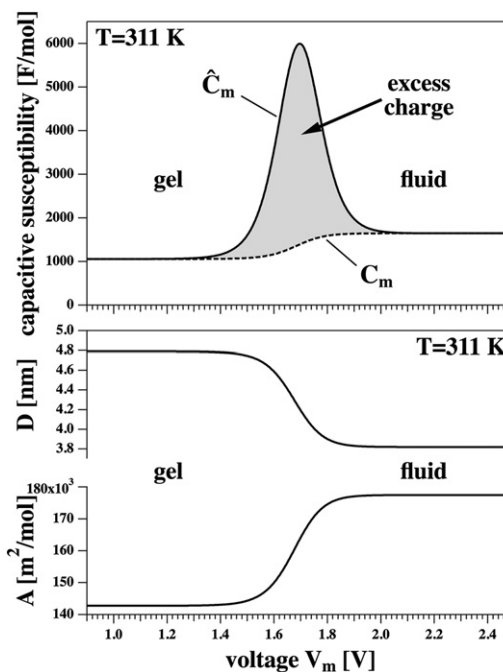


FIGURE 2 (Bottom) Area and thickness changes as a function of voltage at $T = 311$ K. The temperature, $T = 311$ K, is below the melting point of DPPC in the absence of voltage. (Top) Capacitive susceptibility, \hat{C}_m , of DPPC LUV as a function of voltage. The shaded area indicates the excess charge of the voltage-induced transition. The dashed line is the voltage dependent capacitance, C_m .

\widehat{C}_m displays a maximum at a transition voltage that depends on the experimental temperature. This is shown in Fig. 2 (right) for the case of $T = 311$ K. The units are given in absolute units (per mol of lipid) because the area of the membrane is not constant. For comparison, the specific capacitance in the gel state is $0.74 \mu\text{F}/\text{cm}^2$, and in the fluid state it is $0.93 \mu\text{F}/\text{cm}^2$.

The charge on the capacitor is given by

$$q(V_m, T) = \int_{V_m} \widehat{C}_m dV_m. \quad (19)$$

The charge as a function of voltage is shown in Fig. 3 (left) for various temperatures. One can see that the charge undergoes a stepwise change at the transition voltage. We call this change in charge the “excess charge,” Δq_0 . It is given by (see Eq. 6)

$$\Delta q_0(T) = \int_{V_m} V_m \left(\frac{\partial C_m}{\partial V_m} \right) dV_m, \quad (20)$$

where the integral is from a voltage below to a voltage above the transition. The excess charge corresponds to the shaded peak area in Fig. 2 (top). It has a value of 634 C/mol .

One can also determine the capacitive susceptibility, \widehat{C}_m , and the capacitance, C_m , as functions of temperature. This is shown in Fig. 3 (right) for several voltages. For $V_m = 0$, the capacitive susceptibility and the capacitance are identical.

Fluctuations

The heat capacity of a membrane at constant pressure is the temperature derivative of the mean enthalpy and is given by

$$c_p = \frac{d\langle H \rangle}{dT}$$

with

$$\langle H \rangle = \frac{\sum_i H_i \exp(-H_i/kT)}{\sum_i \exp(-H_i/kT)}, \quad (21)$$

where $\langle H \rangle$ is the statistical mean of the enthalpy averaged over all possible microstates of the system with enthalpy H_i . The enthalpies of the microstates are given by

$$H_i = E_i + pV_i + \Pi A_i + \Psi q_i + \dots \quad (22)$$

with the intensive variables pressure p , lateral pressure Π , electrostatic potential Ψ , and the conjugated extensive quantities of internal energy E_i , volume V_i , area A_i , and charge q_i .

Equation 21 immediately leads to

$$c_p = \frac{d\langle H \rangle}{dT} = \frac{\langle H^2 \rangle - \langle H \rangle^2}{kT^2}, \quad p, \Pi, \Psi, \dots = \text{const.}, \quad (23)$$

which is one of the fluctuation relations. Similar relations are found for the specific isothermal volume compressibility κ_T^V , and the area compressibility κ_T^A (23):

$$\kappa_T^V = -\frac{1}{\langle V \rangle} \left(\frac{d\langle V \rangle}{dp} \right)_T = \frac{\langle V^2 \rangle - \langle V \rangle^2}{\langle V \rangle kT}, \quad T, \Pi, \Psi, \dots$$

$$= \text{const.} \quad (24)$$

$$\kappa_T^A = -\frac{1}{\langle A \rangle} \left(\frac{d\langle A \rangle}{d\Pi} \right)_T = \frac{\langle A^2 \rangle - \langle A \rangle^2}{\langle A \rangle kT}, \quad T, p, \Psi, \dots$$

$$= \text{const.} \quad (25)$$

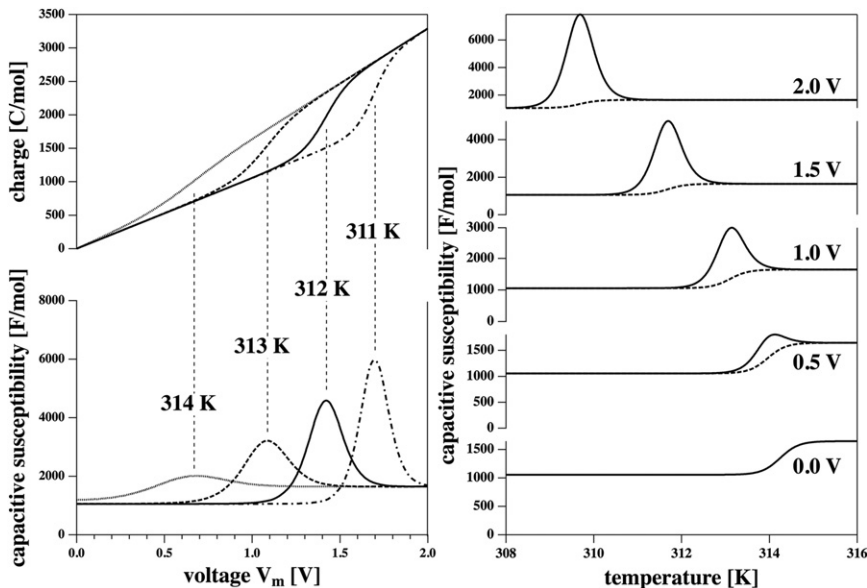


FIGURE 3 (Left) Voltage-induced transition of DPPC LUVs at four different (constant) temperatures. (Top panel) The charge as a function of voltage. (Bottom panel) Capacitive susceptibility as a function of voltage. (Right) Capacitive susceptibility \widehat{C}_m as a function of temperature for five different voltages. The dashed lines represent capacitance C_m as a function of temperature.

Like the heat capacity, these compressibilities have maxima in the melting transition (23).

The capacitive susceptibility of the membrane, \widehat{C}_m , is a similar susceptibility and can be written as

$$\begin{aligned}\widehat{C}_m &= -\frac{dq}{d\Psi} = \frac{dq}{dV_m} = \frac{\langle q^2 \rangle - \langle q \rangle^2}{kT}, \quad T, p, \Pi, \dots \\ &= \text{const.}\end{aligned}\quad (26)$$

All of the above susceptibilities are derivatives of extensive variables with respect to the conjugated intensive variables. For such susceptibilities, the fluctuations $\langle X^2 \rangle - \langle X \rangle^2$ are quadratic forms and therefore always positive. Heat capacity, volume and area compressibility, and capacitance must always be positive definite functions. For this reason, one also finds that the integrals of the susceptibilities are always positive:

$$\begin{aligned}\Delta H &= \int_{T_1}^{T_2} c_p dT > 0 \quad \text{for } T_2 > T_1, \\ -\Delta V &= \int_{p_1}^{p_2} \langle V \rangle \kappa_T^V dp > 0 \quad \text{for } p_2 > p_1, \\ -\Delta A &= \int_{\Pi_1}^{\Pi_2} \langle A \rangle \kappa_T^A d\Pi > 0 \quad \text{for } \Pi_2 > \Pi_1, \\ \Delta q &= \int_{V_{m,1}}^{V_{m,2}} \widehat{C}_m dV_m > 0 \quad \text{for } V_{m,2} > V_{m,1}.\end{aligned}\quad (27)$$

This implies that an increase in voltage across a membrane must result in an increase in charge so long as intensive variables other than V_m are kept constant. This is in agreement with the findings in Fig. 3 (left).

For derivatives of extensive quantities with respect to nonconjugated quantities, the fluctuations are no longer positive definite forms, and negative values can be obtained. For instance, the volume expansion coefficient is given by $d\langle V \rangle/dT = [\langle V H \rangle - \langle V \rangle \langle H \rangle]/kT^2$. For water at 0°C it is negative. Similarly, derivatives of other extensive variables with respect to nonconjugated intensive variables, such as $d\langle q \rangle/dT$ or $d\langle q \rangle/d\Pi$, can also be negative (see below).

Piezoelectricity

A material is said to be ‘‘piezoelectric’’ if the application of a force produces an electric field (and vice versa). ‘‘Piezo’’ originates from the Greek word for pressure, and we will therefore use the term ‘‘piezoelectric’’ as synonymous with ‘‘electromechanical’’ in the sense of pressure-induced voltages across membranes. At fixed temperature,

$$dq = \left(\frac{\partial q}{\partial V_m} \right)_{\mathcal{F}} dV_m + \left(\frac{\partial q}{\partial \mathcal{F}} \right)_{V_m} d\mathcal{F}, \quad (28)$$

where \mathcal{F} is the force normal to the membrane. Because thickness changes in the melting transition are coupled to area changes, this leads to the relation

$$\begin{aligned}dq &= \left(\frac{\partial q}{\partial V_m} \right)_{\mathcal{F}} dV_m + \left(\frac{\partial q}{\partial \Pi} \right)_{V_m} \underbrace{\left(\frac{\partial \Pi}{\partial \mathcal{F}} \right)_{V_m} d\mathcal{F}}_{d\Pi} \\ &= \left(\frac{\partial q}{\partial V_m} \right)_{\Pi} dV_m + \left(\frac{\partial q}{\partial \Pi} \right)_{V_m} d\Pi,\end{aligned}\quad (29)$$

where Π is the lateral pressure of the membrane. In the following we will focus on lateral pressure changes.

At constant voltage, the enthalpy change, $\Delta H(T)$, of the membrane at temperature T due to a lateral pressure is given by a modified version of Eq. 13,

$$\Delta H(V_m, T, \Pi) = \Delta H_0(T) + \Delta W_c(V_m) + \Delta W_A(\Pi), \quad (30)$$

$$\Delta W_A(\Pi) = \Pi \Delta A = \Pi \gamma^A \Delta H_0(T), \quad (31)$$

where $\Delta W_A(\Pi)$ is the work done to change the area of the membrane from A_g to A . With the help of Eq. 14, this leads to

$$\begin{aligned}\Delta H(V_m, T, \Pi) &= \Delta H_0(T) \left(1 + \frac{1}{2} \epsilon_0 \epsilon \gamma_D V_m^2 \frac{A_{gel}}{D_{gel}^2} \left[1 - \frac{1}{2} \right. \right. \\ &\quad \left. \left. \times \left(\frac{\gamma_A}{A_{gel}} + 2 \frac{\gamma_D}{D_{gel}} \Delta H_0(T) \right) \right] + \gamma^A \Pi \right),\end{aligned}\quad (32)$$

and the melting temperature is given by

$$T_m = \frac{\Delta H(V_m, \Pi)}{\Delta S_0} = (1 + \alpha V_m^2 + \gamma^A \Pi) T_{m,0}, \quad (33)$$

with $\alpha = -0.003634$ [1/V²] (see Eq. 15), and $\gamma_A = 0.89$ m²/J.

The charge on a membrane at temperature T , voltage V_m , and lateral pressure Π can be written as

$$q(V_m, T, \Pi) = \epsilon \epsilon_0 \frac{A_{gel} + \Delta A(V_m, T, \Pi)}{D_{gel} + \Delta D(V_m, T, \Pi)} V_m, \quad (34)$$

where ΔA and ΔD are again proportional to ΔH (see Eq. 32).

Now we can determine 1), how the charge on the capacitor changes with changes in lateral pressure at constant voltage and temperature (and vice versa); and 2), how the voltage changes at constant temperature and constant charge with changes in lateral pressure (and vice versa). Fig. 4 (left) shows case 1 for a fixed voltage of $V_m = 1$ V and $T = 315$ K. Under these conditions, the membrane is in the fluid state when the lateral pressure Π is zero. Increasing pressure

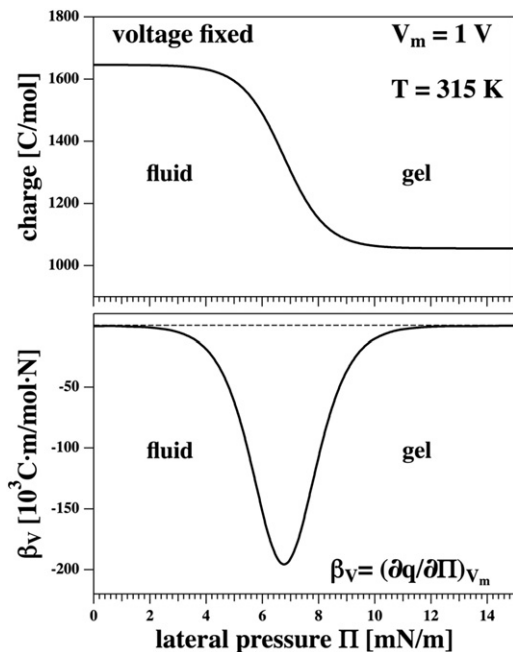


FIGURE 4 Changes in electrical properties induced by lateral pressure changes. (Top) Change in the charge on a capacitor upon changes in lateral pressure at fixed voltage of $V_m = 1$ V. (Bottom) Change in voltage induced by lateral pressure changes at fixed charge on the capacitor ($C_m = 1430.7$ C/mol corresponding to the charge on the fluid phase membrane at $V_m = 1$ V). Increasing lateral pressure renders the membrane more solid.

renders the membrane more solid and the capacitance of the membrane decreases. This leads to a release of charge from the capacitor (i.e., pressure-induced capacitive currents). One can define the corresponding susceptibility,

$$\beta_v \equiv \left(\frac{\partial q}{\partial \Pi} \right)_{V_m}, \quad (35)$$

which is shown in Fig. 4 (right). This susceptibility represents the change in the charge on the membrane due to an increment in the pressure at constant voltage. Because it is a derivative of the extensive variable q with respect to the non-conjugated extensive variable Π , it can have a negative value.

When the charge in Eq. 28 is kept constant ($dq = 0$), we obtain

$$dV_m = \left[- \frac{\left(\frac{\partial q}{\partial \Pi} \right)_{V_m}}{\left(\frac{\partial q}{\partial V_m} \right)_{\Pi}} \right] d\Pi \equiv \beta_q d\Pi. \quad (36)$$

This is shown in Fig. 5 (left) where the charge is fixed at $q = 1645.4$ C/mol, which is the charge on the fluid membrane at a voltage of $V_m = 1$ V. The work done on the membrane by pressure is converted into work done on the charges by changing their distance. Increasing pressure at fixed charge leads to a larger voltage across the membrane. We call this “a piezoelectric effect”. The coupling constant,

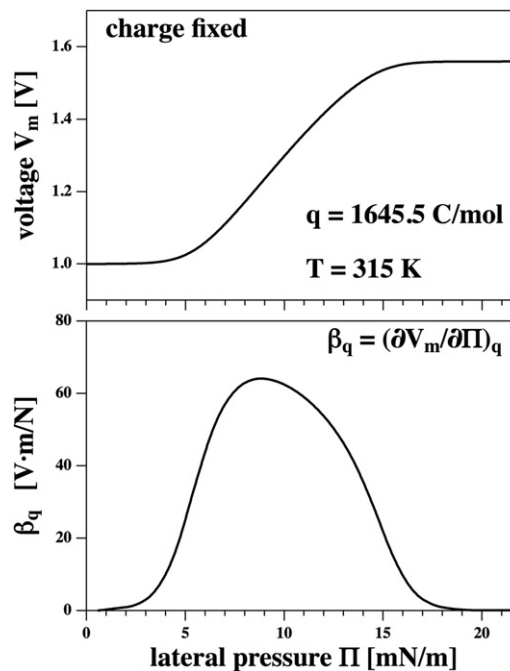


FIGURE 5 (Top) Change in voltage induced by lateral pressure changes at fixed charge on the capacitor ($C_m = 1430.7$ C/mol corresponding to the charge on the fluid phase membrane at $V_m = 1$ V). Increasing lateral pressure renders the membrane more solid. (Bottom) The corresponding susceptibility, $\beta_q = (\partial V_m / \partial \Pi)_q$.

$$\beta_q = \left(\frac{\partial V_m}{\partial \Pi} \right)_q, \quad (37)$$

is shown in Fig. 5 (right). It is identical to the term in rectangular brackets in Eq. 36. A situation of constant charge could be present in a membrane during a sudden reversible change in lateral pressure when charges have no time to dissociate.

DISCUSSION

Lipid membranes are thin capacitors that are unique in their property to display transitions in capacitance. Here, we have offered a theoretical framework for describing the capacitance and the capacitive susceptibility of membranes in the transition regime. Because biomembranes are close to such transitions, this is of immediate biological relevance. Charges on membranes create forces on the membrane that tend to compress the membrane normal to the membrane surface. This effect is called electrostriction (27). It leads to a lowering of the melting temperature of the membrane. Therefore, a change of transmembrane voltage can induce melting transitions. As a consequence, there is an excess charge linked to the voltage-induced transition. This is expressed by the capacitive susceptibility, $\hat{C}_m = \partial q / \partial V_m$, which displays a pronounced maximum at the transition. This behavior is very similar to that of the

heat capacity as a function of temperature and the volume and area compressibilities as a function of hydrostatic and lateral pressure. These functions are all derivatives of extensive thermodynamic variables with respect to their conjugated intensive variable. Using the fluctuation theorem, we have shown that the capacitive susceptibility is related to fluctuations in charge and must therefore always be positive. The maximum of the capacitive susceptibility describes the fact that, in particular voltage regimes close to transitions, a small change in voltage may lead to a large uptake of charge, i.e., the membrane is very susceptible to small variations in conditions.

We further show that electromechanical couplings exist in lipid membranes. One finds a straightforward connection between lateral pressure and the charge on a membrane (at constant voltage) that also assumes a maximum in the melting transition of the membrane. This implies that changes in pressure can give rise to capacitive currents. This effect is described by the derivative of an extensive variable (charge) with respect to a nonconjugated variable (lateral pressure). Such susceptibilities may have either positive or negative values. At constant charge, a coupling also exists between voltage and lateral pressure. This effect corresponds to piezoelectricity. The coupling constant assumes a maximum in the melting transition. This effect is very important for excitatory processes (for instance nerve pulse) and is discussed below. In this article, we have not considered other potentially significant effects such as field-induced changes in polarization. Such effects are relevant and clearly exist in lipid monolayers. This will be the focus of a future publication.

Due to their different capacitance, gel and fluid membranes carry different charges when a constant voltage is applied. An interesting consequence is that the presence of a transmembrane voltage will lead to charge separation in the melting regime where gel and fluid domains coexists. If the membranes contain a fraction of charged lipids, this will lead to an asymmetric accumulation of charged lipids in the fluid domains. Thus, the shape of phase diagrams will be influenced by the application of an electrical field across the membrane. Not surprisingly, in addition to temperature, pressure, and components' concentrations, the transmembrane voltage is also a variable that determines phase diagrams and should be included in Gibbs' phase rule.

The influence of voltage on the capacitance of black lipid membranes had been investigated both theoretically and experimentally in several studies in the 1970s (30,31, 34–36). All of these studies assume that electrostriction is the dominant effect leading to a reduction in membrane thickness and an increase in area due to an increase in voltage. Those studies were done far away from the phase transitions temperature of black lipid membranes. In agreement with our derivations here, they found that the dependence of the capacitance should be a quadratic function of voltage, i.e., $C_m \propto (1 + \alpha V_m^2)$, where α is a constant.

This constant is strongly influenced by the presence of solvent in the black lipid membranes (32). Solvent-free membranes display a much smaller voltage dependence of the capacitance on voltage. In an interesting experimental study, Alvarez and Latorre (30) found that changes in capacitance in asymmetric membranes are influenced by a resting potential, E_0 , such that $C_m \propto (1 + \alpha(V - E_0)^2)$. Alvarez and Latorre discussed this finding in the context of nerve pulse propagation and the measurement of gating currents. They suggested that the membrane itself could display capacitive currents similar to gating currents. What we regard as the novel aspect of the work presented in this article is the recognition of the profound effect that the melting transition has on the nonlinear behavior of the membrane capacitance. Whereas previous authors have assumed a constant compressibility of the membrane, we have made use of the fact that the compressibility is dramatically increased in transitions.

The two terms of the capacitive current, $C_m \cdot dV_m/dt$ and $V_m \cdot dC_m/dt$, in Eq. 3 can have different time dependences. The first term is fast and is largely determined by the electrical resistance of the aqueous medium. The second term has a timescale given by the relaxation time of the membrane, which is slow in transitions. It should therefore be possible to distinguish the two contributions to the capacitive current experimentally. We have previously shown that relaxation timescales can be as large as 30 s for artificial membranes at the transition maximum, and we estimate timescales of up to 100 ms for biomembranes (37,38). Besch et al. (39) investigated HEK293 cells and found currents with timescales in the 10-ms regime after voltage change, which indicates that these currents are related to time-dependent changes in membrane geometry rather than being caused by charging a membrane with a constant capacitance. Slow capacitive currents after voltage changes were also found in rat nerves (40) but interpreted as gating currents.

The electromechanical aspect of membranes has received considerable interest in the past. Ochs and Burton (15) showed in 1974 that black lipid membranes made of egg-PC and cholesterol show electromechanical behavior under voltage-clamp conditions. They applied an oscillating pressure difference across the membrane and recorded capacitive currents that they described by $I_C = V_m \cdot dC_m/dt$ (see Eq. 3).

As mentioned above, the interesting issue of polarization has not been treated here. However, much of the literature on electromechanical phenomena in membranes is dedicated to polarization caused by membrane curvature. Meyer (41) proposed in 1969 that liquid crystals of molecules that possess electrical dipole moments should also be piezoelectric. In particular, Meyer stated that “another possible application of these effects may be in interpreting some of the potentials and ion distributions observed in liquid-crystalline biological structures.” Following this idea, Petrov

(42,43) proposed that membranes should also display piezoelectric behavior. Lipid monolayers have significant dipole moments due to the polar headgroups and the oriented associated water layer. For a symmetric membrane of a zwitterionic lipid, the polarizations of the two layers should cancel because they have opposite orientations.

However, in the presence of curvature, this symmetry argument does not apply, and one expects an electrical field generated by curved membranes. Petrov named this phenomenon “flexoelectricity” and demonstrated the effect in experiments similar to those by Ochs and Burton (15) but interpreted differently as curvature-induced polarization (44,45). In several further articles the authors applied the concept of flexoelectricity to biomembranes and proposed a coupling of flexoelectricity to ionic currents through channel proteins (46,47). Because lipid membranes in the absence of proteins also display ion-channel-like characteristics close to transitions (48–50), Petrov’s considerations are also valid here. It is reasonable to expect that the polarization, P , of membranes changes significantly in the phase transition regime and that the related susceptibility, dP/dE (with E being the electrical field), should have a maximum in the transition. This must be so because the dipole moment of a gel monolayer differs from that of a fluid monolayer. Upon membrane bending one should find an asymmetric distribution of gel and fluid lipids in the two opposing monolayers (51) leading to an effective polarization of the membrane. Unfortunately, we are not aware of any reliable experimental data or theoretical estimates of the magnitude of this polarization.

To our knowledge, the above authors did not investigate the effect of the phase transition on flexoelectricity. However, polarizations induced by curvature are completely analogous to voltage changes induced by lateral compression as described above by Eq. 36 and Fig. 5. Interestingly, Helfrich (52) investigated the effect of voltage on the phase transition temperature of three-dimensional liquid crystals as early as 1970. He found that the shift of the transition is given by

$$\Delta T_m = \frac{1}{2} T_{m,0} \epsilon_0 \Delta \epsilon E^2 / \Delta H_0 \rho,$$

where $\Delta \epsilon$ is the difference of the dielectric constant between liquid and solid phase, ρ is the density, and E is the electric field. Assuming $E/D = V_m$, this law is analogous to Eq. 15.

It is known experimentally that lipid monolayers have large dipole potentials of ~300 mV—somewhat higher for gel than for fluid phase monofilms (53,54). This is frequently attributed to the dipolar nature of the lipid headgroup and the associated water. One can influence the state of lipid monolayers in experiments by an applied field. At positive voltages a liquid-expanded monolayer becomes more solid, whereas the opposite effect is observed when the field is reversed. This rules out the possibility that the influence of voltage is due to electrostriction (K. Feld, Niels

Bohr Institute, 2012), which is independent of the direction of the field. For membranes, this is less clear. Antonov et al. (55) measured the voltage dependence of the lipid chain melting transition via the effect of voltage on membrane permeability, which displays a maximum at the melting point. For synthetic black lipid membranes made of either DPPC or DPPA (dipalmitoyl phosphatidic acid), they found an increase in melting temperature that was well described by

$$\begin{aligned} T_m(\text{DPPC}) &= 315.4[\text{K}] + 20.5[\text{K/V}] \cdot V_m, \\ T_m(\text{DPPA}) &= 332.8[\text{K}] + 55.1[\text{K/V}] \cdot V_m. \end{aligned} \quad (38)$$

This corresponds to a linear shift of T_m of +1.03 K at $V_m = 50$ mV for DPPC and a shift of 2.75 K for DPPA toward higher temperatures, respectively. This effect is opposed to the trend toward lower temperatures predicted above based on electrostriction, which is in agreement with previous predictions from Sugár (56). However, Antonov’s finding is remarkably close to the calculation of Cotterill (57) made by considering the polarization of the monolayers. The shift of T_m by Antonov was found to be linear within experimental accuracy, as expected from Cotterill’s calculation. We do not believe, however, that the derivation of Cotterill is theoretically sound.

An increase of the transition temperature with increasing voltage poses an interesting theoretical problem. Under such circumstances, the fluid membrane can be made solid by voltage leading to a lower capacitance. This would render the excess capacitive susceptibility in the transition negative, and would result in a negative excess charge. According to the considerations of fluctuations above, this can hold only if there are couplings between the charge on the membrane and nonconjugated intensive variables. It remains to be seen whether the simultaneous change of capacitance and polarization allows for such behavior. However, if this were the case, an increase in voltage could possibly result in a decrease of charge, i.e., in capacitive currents against the applied field. It should also be noted that the publication of Antonov et al. (55) is the only one on voltage-induced shifts in transition temperature of which we are aware, and independent experiments verification would be useful. In this respect, the shift of the quadratic dependence on voltage due to a preexisting polarization found by Alvarez and Latorre (30) might contain the answer to the problem presented in this article. The maximum transition temperature may exist at a resting potential different from zero volts. Thus, the melting-point dependence on voltage may be linear and sign-dependent around zero volts. This suggests that the membranes in the experiments of Antonov were not symmetric. Additional studies of polarized membranes are to be encouraged.

Biological membranes display somewhat different melting characteristics than artificial membranes. Their melting profiles are broader and they contain proteins that

probably do not alter their shape in a transition. Therefore, one expects voltage-induced transitions that are qualitatively similar but not necessarily quantitatively identical. For instance, such effects may play an important role in outer hair cells. Fang et al. (58) and Izumi et al. (59) showed in various publications that the capacitance in outer hair cells displays a pronounced maximum. The shape of the profiles is strikingly similar to the capacitive susceptibility curves in Figs. 2 and 3. The authors called this effect the “nonlinear capacitance” and attributed it to a conformational charge transition in the protein Prestin, which is abundant in outer hair cells and is believed to display piezoelectric behavior (60). However, in the same publications it is also shown that the nonlinear capacitance is strongly influenced by alterations of the lipid composition indicating that some properties of the membrane itself contribute to the apparent maximum in capacitance. It may well be that Iwasa (61) describe a voltage-induced transition in the membrane that is tuned by prestin. Iwasa also found a change in membrane charge upon stretching the hair cells (see Fig. 4). The biological importance of electromechanical coupling in outer hair cells was also discussed by Rabbitt et al. (62) and Sachs et al. (63). In a recent article, Brownell et al. (64) showed that tethers pulled from hair cells contract upon application of a voltage difference across the cell body.

The phenomena discussed in this article are especially important for nerve pulse propagation. A change of the membrane state from fluid to gel will alter the capacitance by ~50% (see Eq. 9). If this change occurs within 0.5 ms (which is the timescale of the rising phase of the nervous impulse), it will generate a significant capacitive current of ~100 $\mu\text{A}/\text{cm}^2$ at a constant voltage of $V_m = 100$ mV. Ionic currents of a similar order of magnitude are central elements in the Hodgkin-Huxley model of the nerve pulse (3) (see Fig. 18 therein). Hodgkin and Huxley calculated net ion currents of ~100–600 $\mu\text{A}/\text{cm}^2$ in the squid axon. In previous publications, we have suggested that the nervous impulse consists of an electromechanical soliton corresponding to a lateral compression of the neuronal membranes (13,18–22). In particular, we have proposed that the membrane undergoes a change in state from fluid to gel and back during the nerve pulse. Thus, in the soliton theory one expects capacitive currents of similar magnitude as the ionic currents in the Hodgkin-Huxley model. If charges cannot dissociate (i.e., no capacitive current), one rather expects changes in transmembrane potential (Fig. 5). The consequence of these nonlinear effects is an electromechanical soliton that can travel along membrane cylinder with a velocity close to the speed of sound with many similarities to the nervous impulse. In fact, Tasaki and co-workers showed in various publications that such mechanical pulses exist (8–12,65). Further support comes from atomic force experiments that show mechanical signals in synapse in phase and proportional to voltage changes (14). Further,

light scattering techniques demonstrate that voltage changes are accompanied by changes in nerve dimensions (66,67).

One might reasonably assume that polarization pulses can also propagate in membranes. In lipid monolayers, such pressure pulses have recently been demonstrated experimentally by Griesbauer et al. (68). The pressure pulses are accompanied by voltage pulses that are directly related to and in phase with the pressure pulse (M. F. Schneider, Boston University, private communication, 2012). The coupling displays a maximum in the phase transition regime in an agreement with the concepts proposed here. Such experiments are important and will eventually lead to a complete thermodynamic picture of the capacitive susceptibility and the electromechanical behavior of biomembranes and nerves.

CONCLUSION

We have shown here that lipid membranes are very susceptible to voltage changes close to phase transitions. This result extends previous theoretical and experimental findings of voltage-dependent capacitances of artificial membranes far from such transitions. We have introduced a capacitive susceptibility that displays a pronounced maximum at the transition. These effects depend on other intensive variables. Higher lateral pressure and lower temperature shift the voltage-induced transition toward higher voltages. Voltage changes generate changes in area that result in an electromechanical coupling. Because biomembranes exist naturally in a state close to a transition, this effect will play a role in excitatory processes of the cell. One important example is nerve pulse propagation.

I acknowledge communication with Dr. K. Vanselow from Kiel, who explored the influence of voltage on the mechanics of membranes as early as 1963. I thank Prof. A. D. Jackson from the Niels Bohr Institute for critical reading and helpful comments.

The support of the Villum Foundation (Denmark) is gratefully acknowledged.

REFERENCES

1. Hille, B. 1992. *Ionic Channels of Excitable Membranes*. Cambridge University Press, Cambridge, UK.
2. Johnston, D., and S. M. S. Wu. 1995. *Cellular Neurophysiology*. MIT Press, Boston, MA.
3. Hodgkin, A. L., and A. F. Huxley. 1952. A quantitative description of membrane current and its application to conduction and excitation in nerve. *J. Physiol.* 117:500–544.
4. Hodgkin, A. L., and A. F. Huxley. 1952. Currents carried by sodium and potassium ions through the membrane of the giant axon of *Loligo*. *J. Physiol.* 116:449–472.
5. Neumann, E., S. Kakorin, and K. Toensing. 1999. Fundamentals of electroporative delivery of drugs and genes. *Bioelectrochem. Bioenerg.* 48:3–16.
6. Gehl, J. 2003. Electroporation: theory and methods, perspectives for drug delivery, gene therapy and research. *Acta Physiol. Scand.* 177:437–447.

7. Kassahun, B. T., A. K. Murashov, and M. Bier. 2010. A thermodynamic mechanism behind an action potential and behind anesthesia. *Biophys. Rev. Lett.* 5:35–41.
8. Iwasa, K., and I. Tasaki. 1980. Mechanical changes in squid giant axons associated with production of action potentials. *Biochem. Biophys. Res. Commun.* 95:1328–1331.
9. Iwasa, K., I. Tasaki, and R. C. Gibbons. 1980. Swelling of nerve fibers associated with action potentials. *Science.* 210:338–339.
10. Tasaki, I., K. Iwasa, and R. C. Gibbons. 1980. Mechanical changes in crab nerve fibers during action potentials. *Jpn. J. Physiol.* 30:897–905.
11. Tasaki, I., and K. Iwasa. 1982. Further studies of rapid mechanical changes in squid giant axon associated with action potential production. *Jpn. J. Physiol.* 32:505–518.
12. Tasaki, I., K. Kusano, and P. M. Byrne. 1989. Rapid mechanical and thermal changes in the garfish olfactory nerve associated with a propagated impulse. *Biophys. J.* 55:1033–1040.
13. Heimburg, T., and A. D. Jackson. 2005. On soliton propagation in biomembranes and nerves. *Proc. Natl. Acad. Sci. USA.* 102:9790–9795.
14. Kim, G. H., P. Kosterin, ..., B. M. Salzberg. 2007. A mechanical spike accompanies the action potential in mammalian nerve terminals. *Biophys. J.* 92:3122–3129.
15. Ochs, A. L., and R. M. Burton. 1974. Electrical response to vibration of a lipid bilayer membrane. *Biophys. J.* 14:473–489.
16. Raphael, R. M., A. S. Popel, and W. E. Brownell. 2000. A membrane bending model of outer hair cell electromotility. *Biophys. J.* 78:2844–2862.
17. Petrov, A. G. 2006. Electricity and mechanics of biomembrane systems: flexoelectricity in living membranes. *Anal. Chim. Acta.* 568:70–83.
18. Heimburg, T., and A. D. Jackson. 2007. On the action potential as a propagating density pulse and the role of anesthetics. *Biophys. Rev. Lett.* 2:57–78.
19. Heimburg, T., and A. D. Jackson. 2008. Thermodynamics of the nervous impulse. In *Structure and Dynamics of Membranous Interfaces*. K. Nag, editor. Wiley, New York. 317–339.
20. Andersen, S. S. L., A. D. Jackson, and T. Heimburg. 2009. Towards a thermodynamic theory of nerve pulse propagation. *Prog. Neurobiol.* 88:104–113.
21. Vargas, E. V., A. Ludu, ..., T. Heimburg. 2011. Periodic solutions and refractory periods in the soliton theory for nerves and the locust femoral nerve. *Biophys. Chem.* 153:159–167.
22. Lautrup, B., R. Appali, ..., T. Heimburg. 2011. The stability of solitons in biomembranes and nerves. *Eur. Phys. J E Soft Matter.* 34:1–9.
23. Heimburg, T. 1998. Mechanical aspects of membrane thermodynamics. Estimation of the mechanical properties of lipid membranes close to the chain melting transition from calorimetry. *Biochim. Biophys. Acta.* 1415:147–162.
24. Ebel, H., P. Grabitz, and T. Heimburg. 2001. Enthalpy and volume changes in lipid membranes. I. The proportionality of heat and volume changes in the lipid melting transition and its implication for the elastic constants. *J. Phys. Chem. B.* 105:7353–7360.
25. Heimburg, T., and A. D. Jackson. 2007. The thermodynamics of general anesthesia. *Biophys. J.* 92:3159–3165.
26. Carius, W. 1976. Voltage dependence of bilayer membrane capacitance. *J. Coll. Interf. Sci.* 57:301–307.
27. Vanselow, K. 1966. Studies on the electrostatic-mechanical forces of the nerve membrane upon stimulation of the action potential. [Untersuchungen über die elektrostatisch-mechanischen kräfte an der nervenmembran bei der auslösung des aktionspotentials]. *Z. Dt. Gesellsch. Med. Biol. Elektronik.* 11:1–5.
28. Reference deleted in proof.
29. Heimburg, T. 2007. *Thermal Biophysics of Membranes*. Wiley VCH, Berlin, Germany.
30. Alvarez, O., and R. Latorre. 1978. Voltage-dependent capacitance in lipid bilayers made from monolayers. *Biophys. J.* 21:1–17.
31. White, S. H. 1974. Letter: Comments on “electrical breakdown of bimolecular lipid membranes as an electromechanical instability”. *Biophys. J.* 14:155–158.
32. Requena, J., D. A. Haydon, and S. B. Hladky. 1975. Letter: Lenses and the compression of black lipid membranes by an electric field. *Biophys. J.* 15:77–81.
33. Farrell, B., C. Do Shope, and W. E. Brownell. 2006. Voltage-dependent capacitance of human embryonic kidney cells. *Phys. Rev. E.* 73:041930.
34. White, S. H. 1970. A study of lipid bilayer membrane stability using precise measurements of specific capacitance. *Biophys. J.* 10:1127–1148.
35. White, S. H., and T. E. Thompson. 1973. Capacitance, area, and thickness variations in thin lipid films. *Biochim. Biophys. Acta.* 323:7–22.
36. White, S. H., and W. Chang. 1981. Voltage dependence of the capacitance and area of black lipid membranes. *Biophys. J.* 36:449–453.
37. Grabitz, P., V. P. Ivanova, and T. Heimburg. 2002. Relaxation kinetics of lipid membranes and its relation to the heat capacity. *Biophys. J.* 82:299–309.
38. Seeger, H. M., M. L. Gudmundsson, and T. Heimburg. 2007. How anesthetics, neurotransmitters, and antibiotics influence the relaxation processes in lipid membranes. *J. Phys. Chem. B.* 111:13858–13866.
39. Besch, S., K. V. Snyder, ..., F. Sachs. 2003. Adapting the Quesant Nomad atomic force microscope for biology and patch-clamp atomic force microscopy. *Cell Biochem. Biophys.* 39:195–210.
40. Kilic, G., and M. Lindau. 2001. Voltage-dependent membrane capacitance in rat pituitary nerve terminals due to gating currents. *Biophys. J.* 80:1220–1229.
41. Meyer, R. B. 1969. Piezoelectric effects in liquid crystals. *Phys. Rev. Lett.* 22:918–921.
42. Petrov, A. G. 1984. Flexoelectricity of lyotropics and biomembranes. *Nuovo Cimento D.* 3:174–192.
43. Petrov, A. G. 2002. Flexoelectricity of model and living membranes. *Biochim. Biophys. Acta.* 1561:1–25.
44. Petrov, A. G., R. L. Ramsey, and P. N. Usherwood. 1989. Curvature-electric effects in artificial and natural membranes studied using patch-clamp techniques. *Eur. Biophys. J.* 17:13–17.
45. Petrov, A. G., and P. N. R. Usherwood. 1994. Mechanosensitivity of cell membranes. Ion channels, lipid matrix and cytoskeleton. *Eur. Biophys. J.* 23:1–19.
46. Petrov, A. G., B. A. Miller, ..., P. N. Usherwood. 1993. Flexoelectric effects in model and native membranes containing ion channels. *Eur. Biophys. J.* 22:289–300.
47. Petrov, A. G. 1997. Charge transfer processes in model and biological membranes: defect and mechano-electric aspects; statics and dynamics. *Mol. Cryst. Liq. Cryst. A.* 292:227–234.
48. Blicher, A., K. Wodzinska, ..., T. Heimburg. 2009. The temperature dependence of lipid membrane permeability, its quantized nature, and the influence of anesthetics. *Biophys. J.* 96:4581–4591.
49. Heimburg, T. 2010. Lipid ion channels. *Biophys. Chem.* 150:2–22.
50. Laub, K. R., K. Witschas, ..., T. Heimburg. 2012. Comparing ion conductance recordings of synthetic lipid bilayers with cell membranes containing Trp channels. *Biochim. Biophys. Acta.* 1818:1123–1134.
51. Ivanova, V. P., and T. Heimburg. 2001. Histogram method to obtain heat capacities in lipid monolayers, curved bilayers, and membranes containing peptides. *Phys. Rev. E.* 63:041914.
52. Helfrich, W. 1970. Effect of electric fields on temperature of phase transitions of liquid crystals. *Phys. Rev. Lett.* 24:201–203.
53. Vogel, V., and D. Möbius. 1988. Local surface potentials and electric dipole moments of lipid monolayers: contributions of the water/lipid and the lipid/air interfaces. *J. Coll. Interf. Sci.* 126:408–420.
54. Lee, K. Y. C., and H. M. McConnell. 1995. Effect of electric field gradients on lipid monolayer membranes. *Biophys. J.* 68:1740–1751.

55. Antonov, V. F., E. Y. Smirnova, and E. V. Shevchenko. 1990. Electric field increases the phase transition temperature in the bilayer membrane of phosphatidic acid. *Chem. Phys. Lipids*. 52:251–257.
56. Sugár, I. P. 1979. A theory of the electric field-induced phase transition of phospholipid bilayers. *Biochim. Biophys. Acta*. 556:72–85.
57. Cotterill, R. M. J. 1978. Field effect on lipid melting. *Phys. Scr*. 18:191–192.
58. Fang, J., C. Izumi, and K. H. Iwasa. 2010. Sensitivity of prestin-based membrane motor to membrane thickness. *Biophys. J*. 98:2831–2838.
59. Izumi, C., J. E. Bird, and K. H. Iwasa. 2011. Membrane thickness sensitivity of prestin orthologs: the evolution of a piezoelectric protein. *Biophys. J*. 100:2614–2622.
60. Iwasa, K. H. 2001. A two-state piezoelectric model for outer hair cell motility. *Biophys. J*. 81:2495–2506.
61. Iwasa, K. H. 1993. Effect of stress on the membrane capacitance of the auditory outer hair cell. *Biophys. J*. 65:492–498.
62. Rabbitt, R. D., H. E. Ayliffe, ..., W. E. Brownell. 2005. Evidence of piezoelectric resonance in isolated outer hair cells. *Biophys. J*. 88:2257–2265.
63. Sachs, F., W. E. Brownell, and A. G. Petrov. 2009. Membrane electromechanics in biology, with a focus on hearing. *MRS Bull*. 34:665–670.
64. Brownell, W. E., F. Qian, and B. Anvari. 2010. Cell membrane tethers generate mechanical force in response to electrical stimulation. *Biophys. J*. 99:845–852.
65. Tasaki, I., and P. M. Byrne. 1990. Volume expansion of nonmyelinated nerve fibers during impulse conduction. *Biophys. J*. 57:633–635.
66. Tasaki, I., A. Watanabe, ..., L. Carnay. 1968. Changes in fluorescence, turbidity, and birefringence associated with nerve excitation. *Proc. Natl. Acad. Sci. USA*. 61:883–888.
67. Rector, D. M., X. Yao, ..., J. S. George. 2009. In vivo observations of rapid scattered light changes associated with neurophysiological activity. In *In Vivo Optical Imaging of Brain Function*. R. D. Frostig, editor. CRC Press, Boca Raton, FL. 143–170.
68. Griesbauer, J., S. Bössinger, ..., M. F. Schneider. 2012. Propagation of 2D pressure pulses in lipid monolayers and its possible implications for biology. *Phys. Rev. Lett*. 108:198103.